Faraday Discussions

Cite this: DOI: 10.1039/c9fd00144a

PAPER

Low temperature radical initiated hydrosilylation of silicon quantum dots

Timothy T. Koh, †[a] Tingting Huang,†[a] Joseph Schwan,[b] Pan Xia,[c] Sean T. Roberts, *[d] Lorenzo Mangolini *[bc] and Ming L. Tang *[ac]

Received 20th December 2019, Accepted 13th January 2020
DOI: 10.1039/c9fd00144a

The photophysics of silicon quantum dots (QDs) is not well understood despite their potential for many optoelectronic applications. One of the barriers to the study and widespread adoption of Si QDs is the difficulty in functionalizing their surface, to make, for example, a solution-processable electronically-active colloid. While thermal hydrosilylation of Si QDs is widely used, the high temperature typically needed may trigger undesirable side-effects, like uncontrolled polymerization of the terminal alkene. In this contribution, we show that this high-temperature method for installing aromatic and aliphatic ligands on non-thermal plasma-synthesized Si QDs can be replaced with a low-temperature, radical-initiated hydrosilylation method. Materials prepared *via* this low-temperature route perform similarly to those created *via* high-temperature thermal hydrosilylation when used in triplet fusion photon upconversion systems, suggesting the utility of low-temperature, radical-initiated methods for creating Si QDs with a range of functional behavior.

Introduction

Silicon is both non-toxic and earth-abundant, making it a highly attractive material for quantum-confined semiconductor structures. However, compared to those of direct gap chalcogenide quantum dots (QDs), the electronic states of silicon QDs remain a subject of sizable debate.[1–5] This is not surprising as the electronic properties of QDs are greatly affected by their surface,[6–9] and yet surface functionalization of Si QDs is a key step in transforming these materials into solution-processable optoelectronics. The strong dependence of the electronic

[a]Department of Chemistry, University of California Riverside, Riverside, CA 92521, USA. E-mail: mltang@ucr.edu
[b]Department of Mechanical Engineering, University of California Riverside, Riverside, CA 92521, USA. E-mail: lmangolini@engr.ucr.edu
[c]Materials Science & Engineering Program, University of California Riverside, Riverside, CA 92521, USA
[d]Department of Chemistry, The University of Texas at Austin, Austin, TX 78712, USA. E-mail: roberts@cm.utexas.edu
† Equal contribution.

properties of Si QDs on their surface ligands stems from Si's ability to form strong, covalent bonds to surface-bound molecules. This is distinct from lead and cadmium-based QDs, which tend to ionically coordinate molecules to their surfaces. In principle, the covalently bonded nature of Si QD surfaces creates the opportunity to rationally employ well-understood, widely-used organo-silicon chemistry to functionalize Si QDs to achieve a range of desired optical and electronic properties.

Thermal hydrosilylation is the most widely used method to functionalize Si QDs. Unfortunately, this reaction has many limitations, including use of high temperatures (150–170 °C), substrate limitations due to the need to incorporate a terminal alkene, and the need for a large excess of reagents to complete functionalization in a reasonable timeframe. In particular, this need for a great excess of alkene or alkyne ligands is undesirable when designer ligands are to be incorporated on Si QD surfaces. As such, it is of practical interest to find conditions to hydrosilylate Si QDs at low temperatures in high yield to broaden the range of ligands that can be attached to Si QD surfaces.

In this work, we examine a radical initiator commonly used for polymerization. While radical initiators have been explored to functionalize both porous and single crystal Si,[10–15] no systematic investigation has been reported for Si QDs. Carroll *et al.* showed that hydrosilylation of Si QDs can be achieved at 140 °C when initiated by 1,1′-azobis-(cyclohexanecarbonitrile) (ABCN) in neat alkene.[16] Similarly, 2,2′-azobis(2-methylpropionitrile) (AIBN)[17–19] and 1,1′-azobis(cyclohexanecarbonitrile) (ACHN)[20] were used at lower temperatures. In all these cases, linear aliphatic molecules were bound to the Si QD surface, and the terminal alkene was used in great excess, usually as a neat solvent. The ability to extend this radical based method to forming covalent bonds between aromatic ligands and Si QDs, similar to forming Si–C bonds homogeneously in solution, will allow greater synergy between functional organic materials and Si QDs.

Here, we show that AIBN catalyzed hydrosilylation of Si QDs with aromatic ligands can be achieved at temperatures as low as 60 °C with aliphatic and aromatic alkenes. This is important for multi-excitonic processes like photon upconversion, where Dexter energy transfer occurs between the QD and the surface-bound ligands.[21–27] Since the efficiency of this short-range energy transfer decays exponentially with increasing distance between the QD donor and molecular acceptor, it is imperative to have both species within 1 nm of each other.[28] We show here that the photon upconversion quantum yield (QY) with anthracene-functionalized Si QD light absorbers (Si:9EA) is comparable for larger Si QDs created by both thermal and radical-initiated hydrosilylation. For smaller Si QDs, the photon upconversion QY is ~3.3%, lower than that achieved with thermal methods.[29]

Results and discussion

Fig. 1 shows our light harvesting scheme in which non-thermal plasma synthesized silicon QDs are functionalized with octadecene (ODE) and 9-vinylanthracene (9VA) ligands under one of two conditions: (1) thermally at high temperature (170 °C), or (2) at a relatively low temperature (60 °C) with an AIBN radical initiator. In doing so, Si QDs functionalized with 9-ethylanthracene (9EA) and octadecane (ODA) are created, abbreviated to Si:9EA. These Si:9EA QDs are

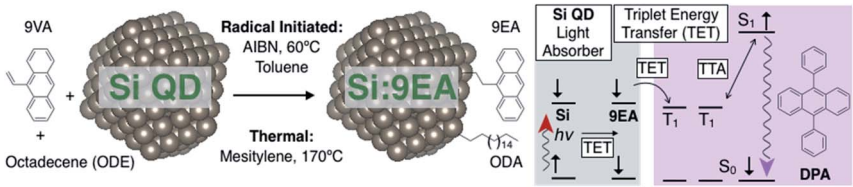

Fig. 1 (Left) Non-thermal plasma-synthesized silicon quantum dots (Si QDs) were hydrosilylated with 9-vinyl anthracene (9VA) and octadecene, to give Si QDs functionalized with 9-ethylanthracene (9EA) and octadecane (Si:9EA). (Right) Si:9EA can photosensitize triplet excited states in diphenylanthracene (DPA) *via* triplet energy transfer (TET). Photon upconversion occurs *via* triplet–triplet annihilation (TTA) between pairs of DPA molecules in their triplet excited states, producing violet light.

colloidally stable in non-polar solvents like toluene or hexane due to the presence of the solubilizing ODA groups. Excitation of Si:9EA QDs creates an excitonic state with triplet character that photosensitizes the surface bound 9EA molecules.[29] This allows for triplet energy transfer (TET) between Si:9EA and diphenylanthracene (DPA) emitter molecules in solution. Photon upconversion is observed when DPA emits from its singlet state following triplet–triplet annihilation between two DPA molecules in their lowest excited triplet state, T_1. Note that direct photoexcitation of a mixture of Si QDs and DPA with light comprised of photons with energy smaller than DPA's 3.2 eV optical gap, such as the 488 nm, 532 nm and 640 nm light used here, does not result in photon upconversion in the absence of surface-bound 9EA on the Si QDs.

Preparation of anthracene functionalized Si QDs

Table 1 outlines the synthetic details. Non-thermal plasma synthesized Si QDs[30] were directly transferred into an air-free glove box to store under nitrogen for future use. Thermal hydrosilylation of Si QDs with 9VA and ODE was performed as previously reported.[29] For the AIBN-initiated radical hydrosilylation of the Si QDs, 0.21 mg of Si QDs were mixed with 0.5 mg of AIBN. Subsequently, either 0.2 or 1.0 mol equivalents of ODE were added, corresponding to 0.03 or 0.144 mL,

Table 1 Synthetic conditions employed for radical-initiated hydrosilylation of Si QDs compared to the conditions previously reported for thermal hydrosilylation. Photoluminescence (PL) spectra were measured in toluene at room temperature with the excitation source set to 532 nm. Photon upconversion measurements were performed with 5.2 mM DPA in toluene at room temperature. Upconversion QYs are reported using a 488 nm CW laser in the linear regime.

Synthesis	AIBN radical initiated: 60 °C, 15 h						Thermal: 170 °C, 3 h			
Sample	RI	RII	RIII	RIV	RV	RVI	T1.5	T2	T3	T4
ODE (mol eq.)	0.2		1.0				4.6			
9VA/ODE (%)	1.25	1.5	0.5	1.5	7.8	15.7	1.50	2.0	3.0	4.0
PL λ_{MAX} (nm)	776	777	774	792	800	804	771	776	784	785
PLQY (%)	12.0	18.3	4.5	2.1	8.4	3.1	11.8	10.4	6.9	5.0
Upconversion QY (%)	0.89	1.13	0.61	0.58	0.25	0.11	0.82	1.57	0.42	0.19

respectively. As shown in Table 1, 9VA was added in different amounts by mole percentage, and the solution was topped up with toluene to the final volume of 0.56 mL. This solution was sealed, stirred and heated in a nitrogen glovebox at 60 °C for 15 hours. In Table 1 and the remainder of this manuscript, Si QDs functionalized *via* radical-initiated or thermal hydrosilylation are labelled as R and T, respectively. There are about 2–3 anthracene ligands per QD.

In the AIBN initiated hydrosilylation, the cloudy solution turned clear, indicating Si QD functionalization. Methanol was used to separate functionalized QDs from free 9VA precursor molecules. 1.7 mL of methanol were added to the reaction solution to precipitate out Si:9EA by centrifugation at 14 000 rpm for 20 min. The precipitated Si:9EA was redispersed in 0.5 mL of toluene, followed by addition of 1.5 mL of methanol and centrifugation at 14 200 rpm for an additional 20 min. This cleaning procedure was repeated three times in total. These cleaning steps resulted in full removal of free 9VA and ODE molecules in solution, as shown by UV-vis absorption spectra of the supernatant which did not show any traces of anthracene. The second pellet was redispersed in toluene, split into two portions, and then precipitated out a third time with 0.75 mL of methanol. One portion was used for upconversion measurements by redispersing it in 0.4 mL of 5.2 mM DPA solution in toluene, while the other portion was saved for characterization.

Fig. 2 shows the electronic absorption and attenuated total reflection infrared (ATR-IR) spectra of Si:9EA colloids synthesized by the AIBN radical-initiated method after cleaning. There is no visible difference compared to the thermally hydrosilylated Si:9EA that we previously reported.[29] For example, vibronic features corresponding to surface-bound anthracene molecules were observed following both synthetic methods. In Fig. 2b, strong C–H absorption from ODA at ~3000 cm^{-1} and C=C aromatic stretching bands from 1600–1700 cm^{-1} are observed, confirming covalent binding of 9EA and ODA to the Si QD surface.

An increase in the amount of 9VA during hydrosilylation bathochromically shifts the photoluminescence (PL) of the Si:9EA QDs. This can be seen in Fig. 3, which plots the PL collected from Si:9EA in toluene following excitation with a 532 nm CW laser. In Fig. 3, we have also highlighted the 9EA triplet energy of

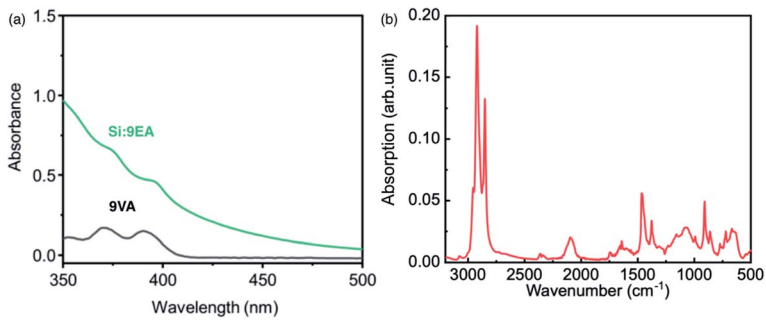

Fig. 2 (a) Absorption spectra of 9VA and Si:9EA QDs hydrosilylated at 60 °C with AIBN radical initiator (green). Vibronic features corresponding to the molecular absorption of the anthracene precursor are observable (black). (b) Attenuated total reflection infra-red (ATR-IR) spectra of Si:9EA showing that octadecane and 9-ethylanthracene (ODA and 9EA) are covalently bound to the surface of the Si QDs.

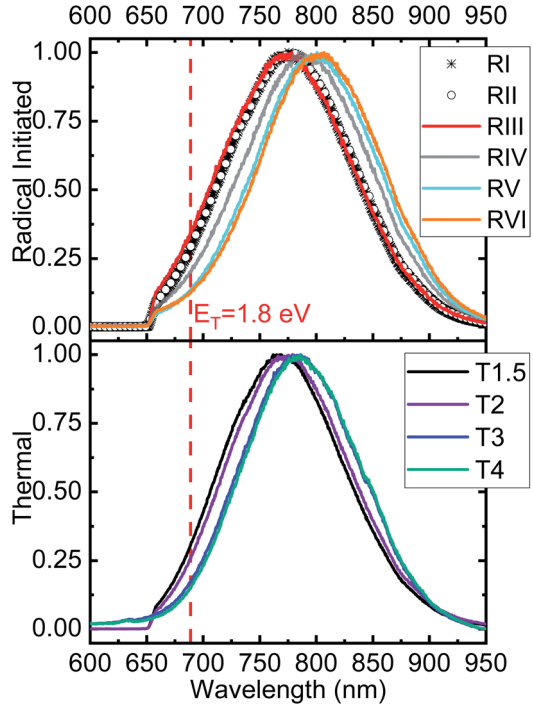

Fig. 3 PL from Si QDs red shifts as the 9VA precursor is increased during hydrosilylation, independent of whether it was initiated by AIBN (top) or thermally performed (bottom). See Table 1 for sample information. Si:9EA was dissolved in toluene and excited using a 532 nm CW laser with a power density of 830 mW cm^{-2} at the sample.

1.8 eV, which falls on the high energy side of the Si QD PL spectrum. Thus, the bathochromic shift could stem from QD size heterogeneity as smaller QDs with a wider bandgaps will energetically favor triplet energy transfer to surface-bound anthracene, leading to quenching of their emission. Consistent with this hypothesis, we observed a narrowing of the Si emission lineshape with increasing 9EA loading. Comparing T1.5 to T4, or the thermally hydrosilylated silicon QDs with 9VA at 1.5% and 4%, respectively, the FWHM of the Si QD PL decreases from 0.27 to 0.24 eV. Similarly, comparing the AIBN initiated radical hydrosilylation samples III to IV with 0.5 and 15.7 mol% of 9VA with respect to ODE, the FWHM decreases from 0.28 to 0.25 eV with 532 nm excitation, too. When the PL traces in Fig. 3 are normalized to their maxima, we also see a decrease in Si QD emission QY with increasing surface concentration of 9VA. Table 1 shows that Si:9EA QD PL decreases by over a factor of two as the amount of surface-bound 9EA increases for the thermal hydrosilylation samples T1.5, T2, T3 and T4. The QY trend is less clear for the AIBN radical-initiated functionalization, possibly due to complication by other surface states, but a net QY decrease with increasing 9EA concentration was seen for the samples we investigated. We note that both radical-initiated and thermal hydrosilylation lead to similar PL shifts with similar 9VA/ODE ratios.

Fig. 4 and 5 (corresponding to samples T2 and RII, respectively) show that the Si PL emitted by Si:9EA blue shifts as the power density of the CW 488 nm, 532 nm

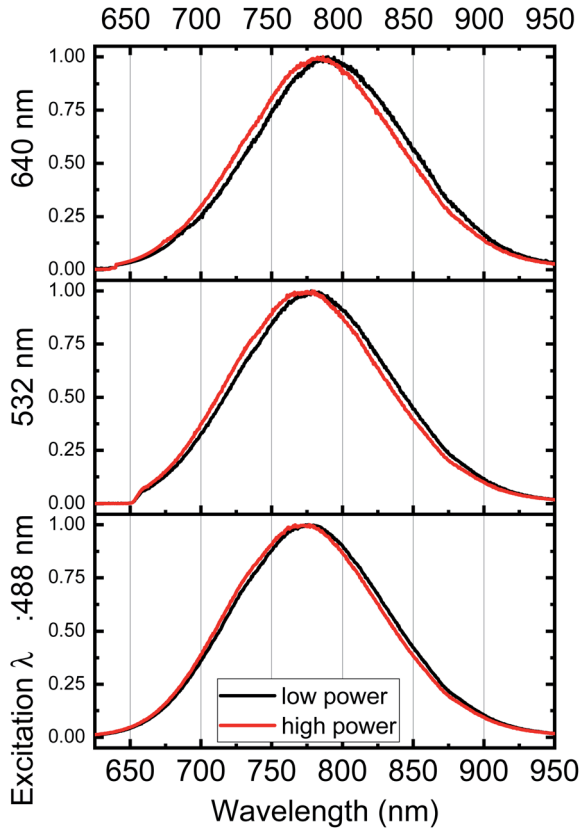

Fig. 4 PL from thermally hydrosilylated Si QDs, Si:9EA (sample T2, Table 1) shows a blue shift as the power density of the 488 nm, 532 nm and 640 nm CW lasers is increased.

and 640 nm lasers increases. This trend is summarized in Table 2. This blue shift could again be attributed to the inhomogeneous size distribution. Gregorkiewicz *et al.* suggested that at high excitation density, smaller Si QDs preferentially emit light as larger Si QDs possess higher extinction cross-sections, making them more susceptible to absorption saturation.[31] Alternatively, there might be a possibility of bi-excitons forming on Si QDs.[32] The fact that blue-shifted emission with increasing excitation density is not observed in direct gap QDs may arise from the long >500 μs lifetimes of Si QDs, compared to the short ~10 ns lifetime of cadmium chalcogenide QDs, or the <10 μs for lead chalcogenide QDs. Time-resolved experiments are needed to differentiate these and other possible scenarios.

Photon upconversion

As shown in Table 1 and Fig. 6, both thermal and radical-initiated hydrosilylation result in photon upconversion QYs between 1.3% and 1.5% for Si QDs whose emission peaks at 780 nm. This PL maximum was obtained for thermally hydrosilylated Si QDs with ODE only when excited with a 488 nm CW laser. Compared to the direct gap chalcogenide QDs, the indirect gap nature of Si QDs

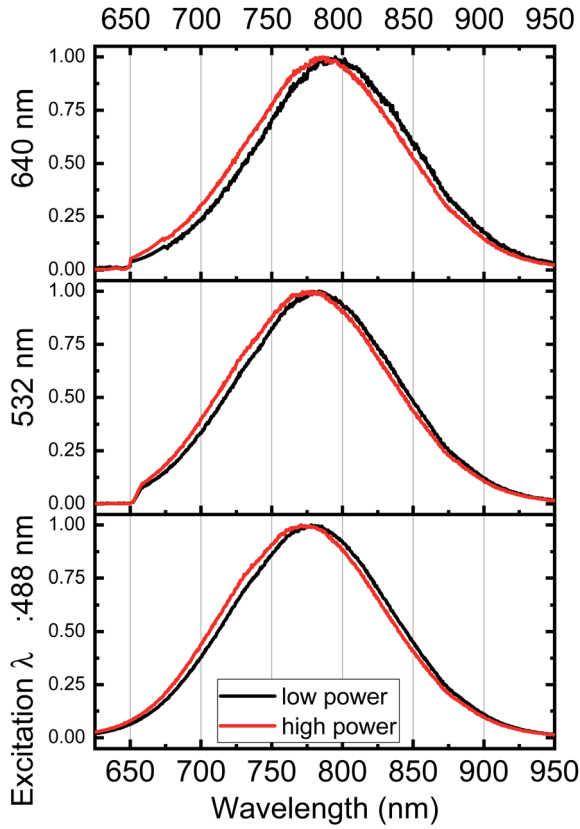

Fig. 5 PL from Si:9EA prepared by AIBN-initiated hydrosilylation of Si QDs (sample RII, Table 1) shows a blue shift as the power density of the 488 nm, 532 nm and 640 nm CW lasers is increased.

makes it impossible to index particle size using electronic absorption spectroscopy. On the other hand, the PL of Si QDs is affected by the synthetic methodology, thus in this work we compare the Si QD size by comparing the PL when thermally hydrosilylated with ODE only is carried out. The photon upconversion QY was determined with a R6G standard as described previously.[29] The photon upconversion QY for the samples in Table 1 is not high as the large size of the Si QDs causes their bandgaps to be too small relative to the T_1 level of 9EA of ~1.8 eV

Table 2 As the excitation density of the CW lasers is increased by 10×, a slight blue shift of the PL of Si:9EA is observed for all excitation wavelengths. Samples T2 (Fig. 4) and RII (Fig. 5) were dissolved in toluene. All measurements were performed at RT

Sample	λ_{EXC} (nm)	488		532		640	
	Power (mW cm^{-2})	100	1800	85	830	18	130
RII	PLQY (%)	32.0	17.2	33.6	18.3	9.6	7.6
	PL λ_{MAX} (nm)	779	774	783	778	795	787
T2	PLQY (%)	16.0	9.9	21.8	11.8	21.2	13.0
	PL λ_{MAX} (nm)	778	774	781	776	791	785

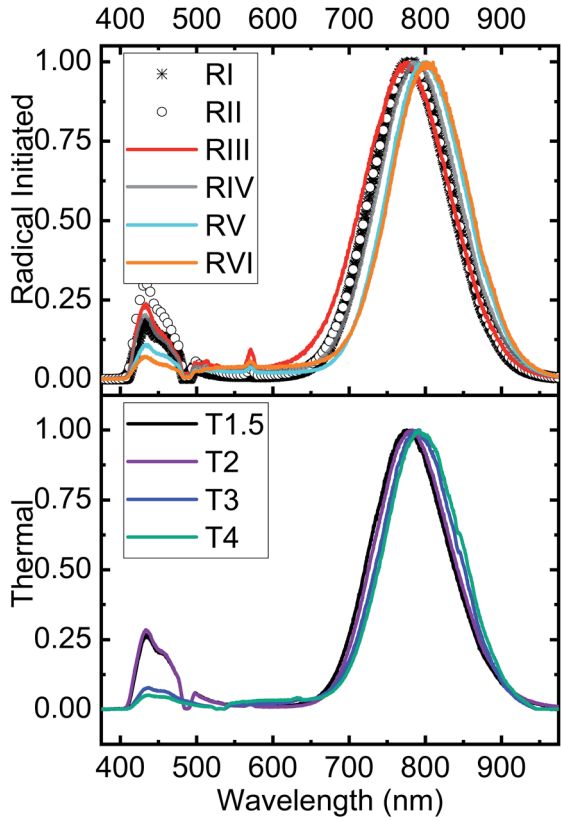

Fig. 6 The photon upconversion observed when Si:9EA colloids from Table 1 were dissolved in 5.2 mM DPA and excited with a 488 nm CW laser.

to allow efficient energy transfer. This makes triplet energy transfer (TET in Fig. 1) a thermodynamically uphill process. Using Si QDs of a smaller size that emit maximally at 700 nm, a photon upconversion QY of 3.34% was obtained. This is a factor of 2 lower than the value we previously reported.[29] This suggests that the heating step at 170 °C may remove some surface states deleterious for triplet energy transfer.

Conclusions

We have shown that functionalization of non-thermal plasma-synthesized silicon QDs can be performed *via* radical-initiated hydrosilylation at low temperature with a substantially lower concentration of ligands. The photon upconversion quantum yields here are a barometer of the efficiency of triplet energy transfer between the Si QD and the surface-bound anthracene, a measure of the quality of the organic–inorganic surface. For larger sized Si QDs, both hydrosilylation methods perform equally well. However, for smaller QDs, the high-temperature thermal hydrosilylation method gives higher photon upconversion QYs compared to the low-temperature radical-initiated route, suggesting size

dependent surface reactivity. The functionalization of Si QDs needs be further developed to enhance electronic communication between the Si semiconductor core and conjugated ligands on its surface.

Conflicts of interest

There are no conflicts to declare.

Acknowledgements

M. L. T. acknowledges National Science Foundation (NSF) grant OISE-1827087 and the Alfred P. Sloan Foundation. L. M. acknowledges support from the NSF under award number 1351386 (CAREER). STR acknowledges support from the NSF (CHE-1610412), the Robert A. Welch Foundation (Grant F-1885), and Research Corporation for Science Advancement (Grant #24489).

References

1 W. de Boer, D. Timmerman, K. Dohnalova, I. N. Yassievich, H. Zhang, W. J. Buma and T. Gregorkiewicz, Red spectral shift and enhanced quantum efficiency in phonon-free photoluminescence from silicon nanocrystals, *Nat. Nanotechnol.*, 2010, **5**, 878–884.
2 K. Dohnalova, A. N. Poddubny, A. A. Prokofiev, W. de Boer, C. P. Umesh, J. M. J. Paulusse, H. Zuilhof and T. Gregorkiewicz, Surface brightens up Si quantum dots: direct bandgap-like size-tunable emission, *Light: Sci. Appl.*, 2013, **2**, e47.
3 W. de Boer, D. Timmerman, I. Yassievich, A. Capretti and T. Gregorkiewicz, Reply to 'Absence of redshift in the direct bandgap of silicon nanocrystals with reduced size', *Nat. Nanotechnol.*, 2017, **12**, 932–933.
4 F. Trojanek, K. Neudert, M. Bittner and P. Maly, Picosecond photoluminescence and transient absorption in silicon nanocrystals, *Phys. Rev. B: Condens. Matter Mater. Phys.*, 2005, **72**, 075365.
5 J. W. Luo, S. S. Li, I. Sychugov, F. Pevere, J. Linnros and A. Zunger, Absence of redshift in the direct bandgap of silicon nanocrystals with reduced size, *Nat. Nanotechnol.*, 2017, **12**, 930–932.
6 N. P. Brawand, M. Voros and G. Galli, Surface dangling bonds are a cause of B-type blinking in Si nanoparticles, *Nanoscale*, 2015, **7**, 3737–3744.
7 A. Puzder, A. J. Williamson, J. C. Grossman and G. Galli, Surface control of optical properties in silicon nanoclusters, *J. Chem. Phys.*, 2002, **117**, 6721–6729.
8 A. Puzder, A. J. Williamson, J. C. Grossman and G. Galli, Surface chemistry of silicon nanoclusters, *Phys. Rev. Lett.*, 2002, **88**, 097401.
9 G. Allan, C. Delerue and M. Lannoo, Nature of luminescent surface states of semiconductor nanocrystallites, *Phys. Rev. Lett.*, 1996, **76**, 2961–2964.
10 J. M. Buriak, Organometallic chemistry on silicon and germanium surfaces, *Chem. Rev.*, 2002, **102**, 1271–1308.
11 C. Chatgilialoglu, Organosilanes as radical-based reducing agents in synthesis, *Acc. Chem. Res.*, 1992, **25**, 188–194.
12 M. R. Linford and C. E. D. Chidsey, Alkyl monolayers covalently bonded to silicon surfaces, *J. Am. Chem. Soc.*, 1993, **115**, 12631–12632.

13 M. R. Linford, P. Fenter, P. M. Eisenberger and C. E. D. Chidsey, Alkyl Monolayers on Silicon Prepared from 1-Alkenes and Hydrogen-Terminated Silicon, *J. Am. Chem. Soc.*, 1995, **117**, 3145–3155.

14 M. Miyano, Y. Kitagawa, S. Wada, A. Kawashima, A. Nakajima, T. Nakanishi, J. Ishioka, T. Shibayama, S. Watanabe and Y. Hasegawa, Photophysical properties of luminescent silicon nanoparticles surface-modified with organic molecules *via* hydrosilylation, *Photochem. Photobiol. Sci.*, 2016, **15**, 99–104.

15 R. Mazzaro, A. Gradone, S. Angeloni, G. Morselli, P. G. Cozzi, F. Romano, A. Vomiero and P. Ceroni, Hybrid Silicon Nanocrystals for Color-Neutral and Transparent Luminescent Solar Concentrators, *ACS Photonics*, 2019, **6**, 2303–2311.

16 G. M. Carroll, R. Limpens and N. R. Neale, Tuning Confinement in Colloidal Silicon Nanocrystals with Saturated Surface Ligands, *Nano Lett.*, 2018, **18**, 3118–3124.

17 A. Angi, M. Loch, R. Sinelnikov, J. G. C. Veinot, M. Becherer, P. Lugli and B. Rieger, The influence of surface functionalization methods on the performance of silicon nanocrystal LEDs, *Nanoscale*, 2018, **10**, 10337–10342.

18 F. Sangghaleh, I. Sychugov, Z. Y. Yang, J. G. C. Veinot and J. Linnros, Near-Unity Internal Quantum Efficiency of Luminescent Silicon Nanocrystals with Ligand Passivation, *ACS Nano*, 2015, **9**, 7097–7104.

19 Z. Y. Yang, C. M. Gonzalez, T. K. Purkait, M. Iqbal, A. Meldrum and J. G. C. Veinot, Radical Initiated Hydrosilylation on Silicon Nanocrystal Surfaces: An Evaluation of Functional Group Tolerance and Mechanistic Study, *Langmuir*, 2015, **31**, 10540–10548.

20 R. T. Anderson, X. Zang, R. Fernando, M. J. Dzara, C. Ngo, M. Sharps, R. Pinals, S. Pylypenko, M. T. Lusk and A. Sellinger, Direct Conversion of Hydride- to Siloxane-Terminated Silicon Quantum Dots, *J. Phys. Chem. C*, 2016, **120**, 25822–25831.

21 Z. Y. Huang, X. Li, M. Mahboub, K. M. Hanson, V. M. Nichols, H. Le, M. L. Tang and C. J. Bardeen, Hybrid Molecule-Nanocrystal Photon Upconversion Across the Visible and Near-Infrared, *Nano Lett.*, 2015, **15**, 5552–5557.

22 Z. Y. Huang and M. L. Tang, Designing Transmitter Ligands That Mediate Energy Transfer between Semiconductor Nanocrystals and Molecules, *J. Am. Chem. Soc.*, 2017, **139**, 9412–9418.

23 M. Wu, D. N. Congreve, M. W. B. Wilson, J. Jean, N. Geva, M. Welborn, T. Van Voorhis, V. Bulovic, M. G. Bawendi and M. A. Baldo, Solid-state infrared-to-visible upconversion sensitized by colloidal nanocrystals, *Nat. Photonics*, 2016, **10**, 31–34.

24 L. Nienhaus, M. F. Wu, N. Geva, J. J. Shepherd, M. W. B. Wilson, V. Bulovic, T. Van Voorhis, M. A. Baldo and M. G. Bawendi, Speed Limit for Triplet-Exciton Transfer in Solid-State PbS Nanocrystal-Sensitized Photon Upconversion, *ACS Nano*, 2017, **11**, 7848–7857.

25 B. Joarder, N. Yanai and N. Kimizuka, Solid-State Photon Upconversion Materials: Structural Integrity and Triplet-Singlet Dual Energy Migration, *J. Phys. Chem. Lett.*, 2018, **9**, 4613–4624.

26 K. Okumura, K. Mase, N. Yanai and N. Kimizuka, Employing Core-Shell Quantum Dots as Triplet Sensitizers for Photon Upconversion, *Chem.–Eur. J.*, 2016, **22**, 7721–7726.

27 C. Mongin, S. Garakyaraghi, N. Razgoniaeva, M. Zamkov and F. N. Castellano, Direct observation of triplet energy transfer from semiconductor nanocrystals, *Science*, 2016, **351**, 369–372.
28 X. Li, Z. Y. Huang, R. Zavala and M. L. Tang, Distance-Dependent Triplet Energy Transfer between CdSe Nanocrystals and Surface Bound Anthracene, *J. Phys. Chem. Lett.*, 2016, **7**, 1955–1959.
29 P. Xia, E. K. Raulerson, D. Coleman, C. S. Gerke, L. Mangolini, M. L. Tang and S. T. Roberts, Achieving spin-triplet exciton transfer between silicon and molecular acceptors for photon upconversion, *Nat. Chem.*, 2020, **12**, 137–144.
30 L. Mangolini and U. Kortshagen, Plasma-assisted synthesis of silicon nanocrystal inks, *Adv. Mater.*, 2007, **19**, 2513–2519.
31 E. M. L. D. de Jong, H. Rutjes, J. Valenta, M. T. Trinh, A. N. Poddubny, I. N. Yassievich, A. Capretti and T. Gregorkiewicz, Thermally stimulated exciton emission in Si nanocrystals, *Light: Sci. Appl.*, 2018, **7**, 17133.
32 M. C. Beard, K. P. Knutsen, P. R. Yu, J. M. Luther, Q. Song, W. K. Metzger, R. J. Ellingson and A. J. Nozik, Multiple exciton generation in colloidal silicon nanocrystals, *Nano Lett.*, 2007, **7**, 2506–2512.